Supporting Information

for

Fe-Doped CuO Embedded in Carbon Nanosheets for Efficient and Selective Nitrate Electroreduction to Ammonia

Jinjie Lin,[a]‡ Nan Wu,[a]‡ Xianhong Wu,[a*] Run-Cang Sun [a*]

[a]Liaoning Key Lab of Lignocellulose Chemistry and BioMaterials, Liaoning Collaborative Innovation Center for Lignocellulosic Biorefinery, College of Light Industry and Chemical Engineering, Dalian Polytechnic University, Dalian 116034, China.

‡These authors contribute equally: Jinjie Lin and Nan Wu

∗Corresponding author. wuxianhong@dlpu.edu.cn; rcsun3@dlpu.edu.cn

Supplementary Text

1. Experimental section

1.1 Chemicals and Catalyst Preparation.

Potassium hydroxide, hydrochloric acid (HCl, 12 mol/L), sodium hypochlorite, ammonium chloride, and boric acid were purchased from Tianjin Kemiou Chemical Reagent Co., Ltd. Gelatin was purchased from Sinopharm Chemical Reagent Co., Ltd. Potassium nitrate, sodium nitrite, nickel chloride, salicylic acid, trisodium citrate dihydrate, sulfamic acid, N-(1-naphthyl)ethylenediamine dihydrochloride, and sodium nitroprusside were purchased from Macklin Chemical Reagent Co., Ltd. Copper chloride, ferric chloride and Nafion 115 membrane were purchased from Aladdin Chemistry Co., Ltd. The deionized water was produced using a Millipore Milli-Q grade. All chemicals were of analytical grade and used without further purification.

The Fe-doped CuO/C catalysts were prepared via a facile evaporation-drying followed by a high-temperature calcination strategy. In a typical procedure, boric acid, gelatin, and metal salts were dissolved in deionized water. The mass ratio of the components was fixed at 10 : 1 : 0.1 : 0.1 (Water : Boric acid : Gelatin : Total metal salts). The mixture was continuously stirred at 85 °C until the solvent was completely evaporated. The resulting solid residue was then transferred to an oven and dried at 60 °C for 12 h. The dried precursor was ground into a fine powder using an agate mortar and subsequently calcined at 650 °C for 2 h in a N_2 atmosphere with a heating rate of 5 °C/min. After cooling to room temperature, the obtained product underwent a reflux treatment in deionized water at 90 °C for 2 h to remove impurities. The suspension was then centrifuged, and the supernatant was decanted. Finally, the precipitate was dried in an oven at 60 °C to obtain the final catalyst.

CuO/C: Prepared using only copper(II) chloride ($CuCl_2$) as the metal precursor.

Fe_1-CuO/C: Prepared using a mixture of iron(III) chloride ($FeCl_3$) and $CuCl_2$ with a mass ratio of 1:1.

Fe_2-CuO/C: Prepared using a mixture of $FeCl_3$ and $CuCl_2$ with a mass ratio of 1:5.

1.2 Structure characterizations

The morphology and composition of the samples were analyzed using field emission

scanning electron microscopy (FESEM, ZEISS-Merlin), transmission electron microscopy (TEM, JEOL-2010) with energy dispersive X-ray spectroscopy (EDX), and high-resolution transmission electron microscopy (HRTEM, JEOL-2010). Aberration-corrected HAADF-STEM images were obtained using a Talos F200X field emission transmission electron microscope with a 200 kV accelerating voltage. X-ray diffraction (XRD) patterns were recorded on a Rigaku device at 40 kV and 40 mA, while X-ray photoelectron spectroscopy (XPS) was employed using a PHI Quantera SXM instrument to analyze the composition and oxidation states of the elements in the samples. In-situ infrared spectra were recorded using ATR-SEIRAS (Attenuated Total Reflection Surface-Enhanced Infrared Absorption Spectroscopy) on a Thermo Scientific Nicolet iS50 FTIR spectrometer with an integrated MCT detector. The chemical states of elements were recorded by XPS.

1.3 Electrochemical measurements

The electrochemical measurements were carried out in both a single-cell and H-type glass cell. In the H-type cell, the cell was separated by a Nafion 115 membrane, and the experiments were conducted at room temperature. A CHI760E workstation was used to record the electrochemical responses. A graphite rod and a Hg/HgO electrode were selected as the counter and reference electrodes, respectively. The hydrogel was directly used as the working electrode. The potential measured via the Hg/HgO electrode was converted to the reversible hydrogen electrode (RHE) potential using the Nernst equation: E(RHE) = E(Hg/HgO) + 0.0591 * pH + 0.098. The linear sweep voltammetry (LSV) curves were established at a scan rate of 5 mV/s, followed by 60 cycles of cyclic voltammetry (CV) tests to obtain stable curves. Chronoamperometry was used to evaluate the stability under different current densities. Electrochemical impedance spectroscopy (EIS) measurements were performed over a frequency range of 0.1-1.0×10^6 Hz, with tests conducted at open circuit potential. The LSV curves are presented without iR correction.

1.4 Determination of ion concentrations

NH_4^+Quantification. The produced NH_3 was quantitatively determined using the indophenol blue method. Typically, 50 μL of electrolyte was withdrawn from the reaction cell and diluted to 2 mL. Then, 2 mL of 1 M KOH solution containing 5 wt% sodium citrate and 5 wt% salicylic acid, along with 1 mL of freshly prepared 0.05 M NaClO solution, were added. The mixed solution was

shaken for a few seconds. Finally, 0.2 mL of a 1 wt.% sodium nitroferricyanide solution was added for the color reaction. After keeping the reaction mixture at room temperature for 1 hour, the resulting solution was measured using an ultraviolet-visible (UV-Vis) spectrophotometer. The absorbance at approximately 655 nm was measured to calculate the concentration of NH_3. To quantify the amount of NH_3, a calibration curve was built using a standard NH_4Cl solution in 0.1 M KOH.

NO_2^- Quantification. A specific color reagent for NO_2^- quantification was prepared by dissolving 0.5 g of sulfamic acid in 50 mL of 2.0 M HCl to obtain solution A. Dissolve 20.0 mg of N-(1-naphthyl)ethylenediamine dihydrochloride in 20 mL of ultrapure water to obtain solution B. Take 2.5 mL of different concentrations of standard solutions, add 2.5 mL of 2.0 M HCl, mix thoroughly, then add 0.1 mL of solution A, mix well, and let it stand for 10 minutes. Then, add 0.1 mL of solution B, mix well, and let it stand for 30 minutes. Perform UV-visible absorption spectroscopy tests within the 650 nm to 400 nm range, and obtain the concentration-absorbance curve based on the absorbance at 540 nm.

1.5 Calculation of the FE and NH_3 yield rate

The FE of electrocatalytic NO_3^--NH_3 conversion and NO_3^--NO_2^- conversion was calculated as follows:

$$FE_{NH3} = C_{NH3} \times V \times N \times F / (Q \times M)$$

C_{NH3}: the measured NH_4^+ concentration (μg mL^{-1}).

V: the volume of the electrolyte (mL).

N: the number of electrons transferred for product formation.

F: Faraday constant, 96485 C mol^{-1}.

Q: total electric charge (C).

M: The relative molecular mass of NH_4Cl, which is 53.5 g mol^{-1}.

$$FE_{NO2} = C_{NO2} \times V \times N \times F / (Q \times M)$$

C_{NO2}: the measured NH_4^+ concentration (μg mL^{-1}).

V: the volume of the electrolyte (mL).

N: the number of electrons transferred for product formation.

F: Faraday constant, 96485 C mol^{-1}.

Q: total electric charge (C).

M: The relative molecular mass of $NANO_2$, which is 68.99 g mol^{-1}.

The calculation method for the yield rate of NH_3 product was calculated as follows:

$$v_{NH3} = (C_{NH3} \times V) / (S \times t) \times 3600$$

v_{NH3}: the yield rate (μg h^{-1} cm^{-2}).

$C_{NH3:}$ the measured NH_4^+ concentration (μg mL^{-1}).

V: the volume of the electrolyte (mL).

S: the area of the catalyst.

t: the reduction reaction time (s).

1.6 The DFT calculation details

The calculations were carried out using the PBE functional within the VASP software package. We utilized the PAW method to model the core-valence interactions. The energy cutoff was set to 500 eV, and spin polarization was included in all calculations to accurately describe the electronic structure. For k-point sampling, a (3 × 3 × 1) mesh was used. We also applied the D3BJ correction to account for van der Waals interactions.The DFT calculations focus on the electronic structure of the catalyst, and the key results, including the energy level diagram and density of states (DOS).

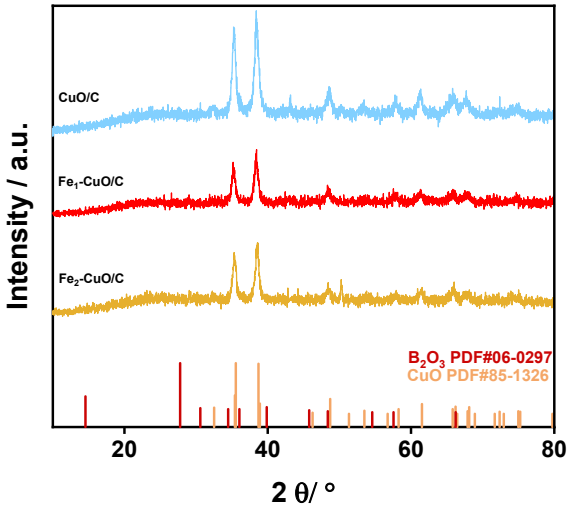

Figure S1. The XRD of the CuO/C, Fe_1-CuO/C and Fe_2-CuO/C.

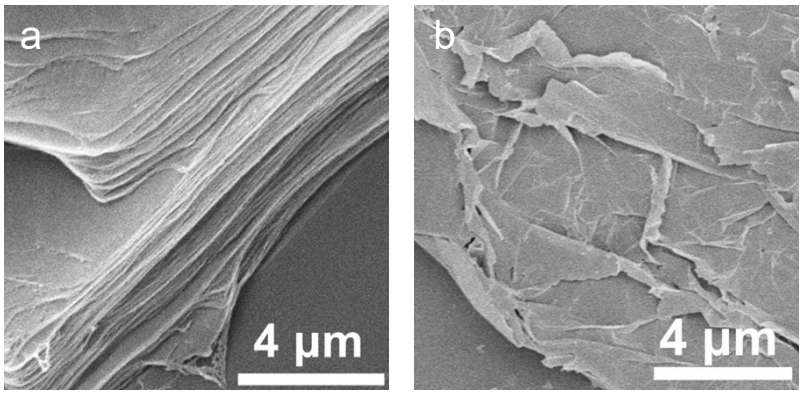

Figure S2. (a) SEM of boric acid nanoplates coated with gelatin/matal salts. (b) SEM images of Fe_1-CuO/C.

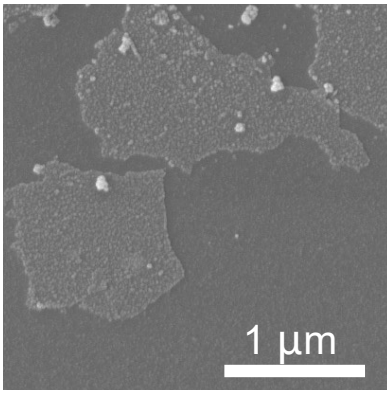

Figure S3. SEM images of Fe_2-CuO/C.

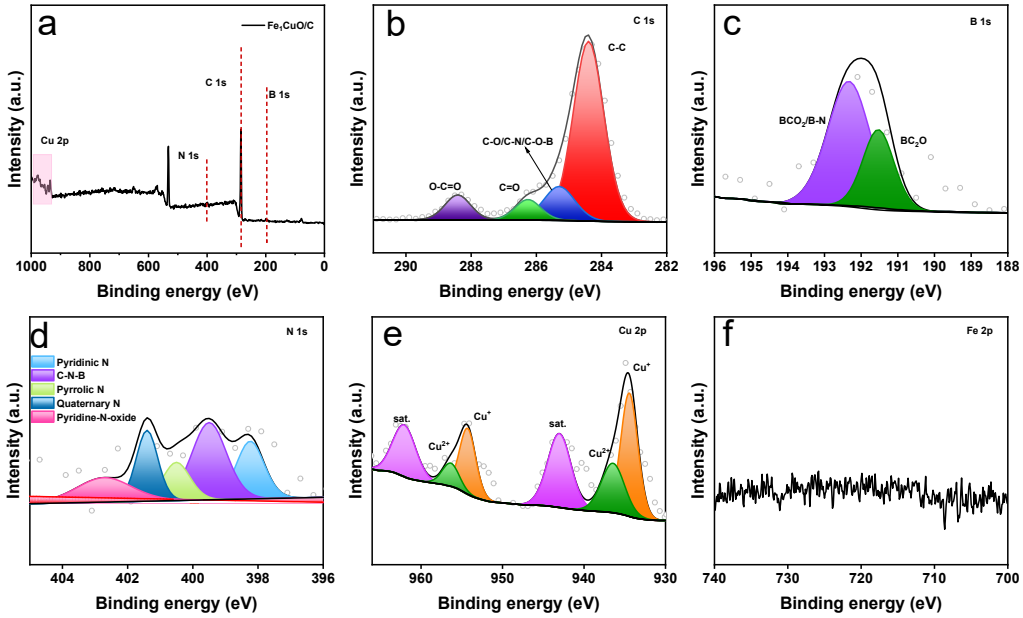

Figure S4. The XPS of Fe_1-CuO/C catalyst. (a) Survey XPS spectrum, (b) C 1s, (c) B 1s , (d) N 1s, (e) Cu 2p, (f) Fe 2p.

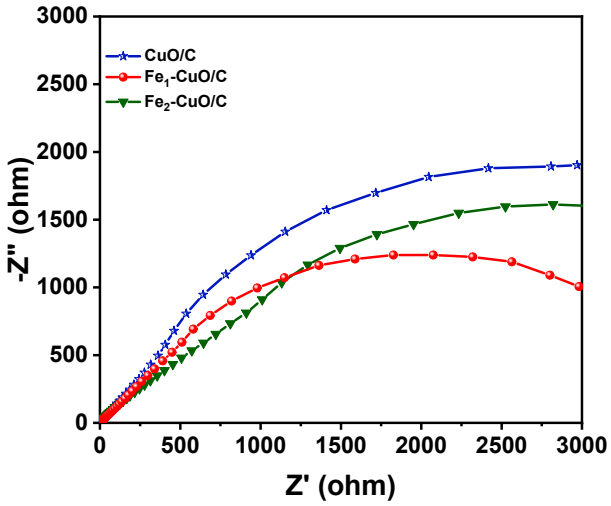

Figure S5. EIS of the CuO/C, Fe_1-CuO/C, and Fe_2-CuO/C electrodes measured.

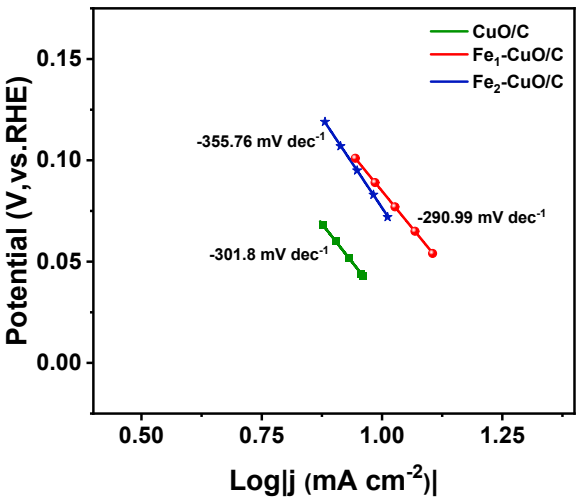

Figure S6. Tafel plots of the Fe_1-CuO/C, Fe_2-CuO/C, and pure CuO/C electrodes derived from their corresponding LSV curves.

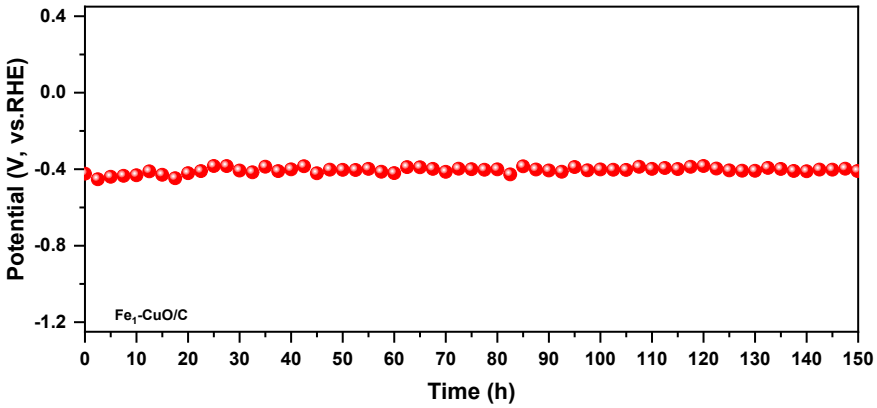

Figure S7. Long-term chronopotentiometry stability test of the Fe_1-CuO/C electrode recorded for 150 hours.

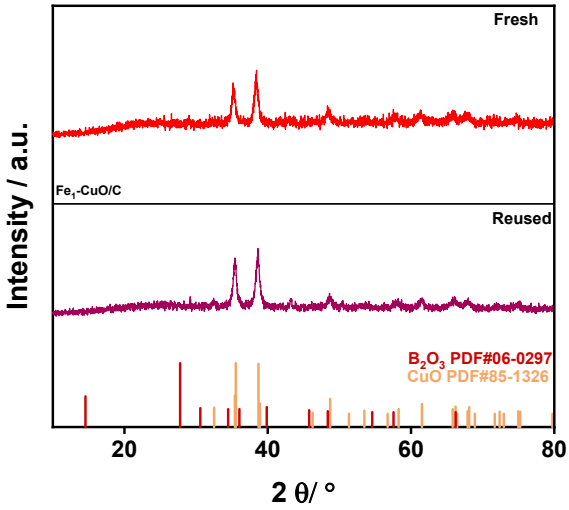

Figure S8. XRD patterns of the Fe_1-CuO/C catalyst before (Fresh) and after (Used) the long-term electrocatalytic NO_3^-RR stability test.

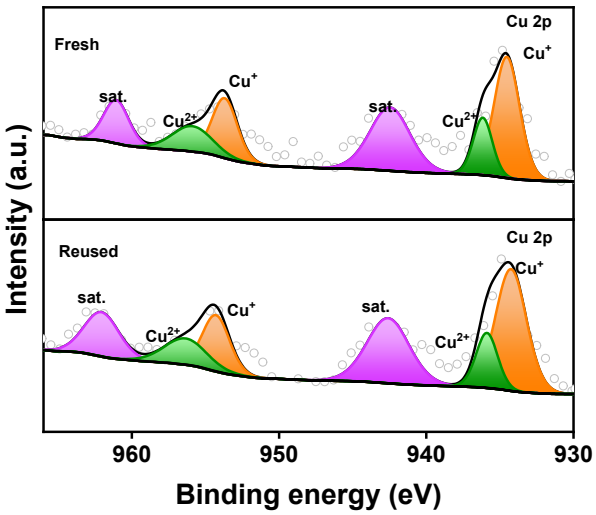

Figure S9. High-resolution XPS spectra of Cu 2p for the Fe_1-CuO/C electrode before and after the stability test.

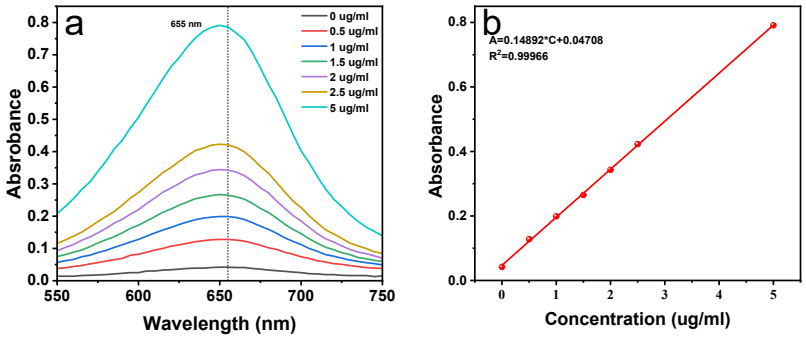

Figure S10. The concentration-absorbance UV-vis calibration curve of NH_3 using different concentration of NH_4Cl solutions as standards. (a) UV-vis curves with NH_4^+ ions and (b) linear fitting results of the calibration curve.

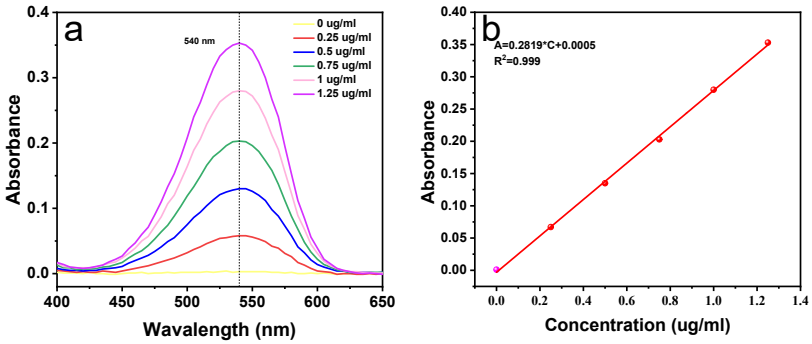

Figure S11. The concentration-absorbance UV-vis calibration curve of NO_2 - using different concentration of KNO_2 solutions as standards. (a) UV-vis curves of assays with NO_2^- ions and (b) linear fitting results of the calibration curve.

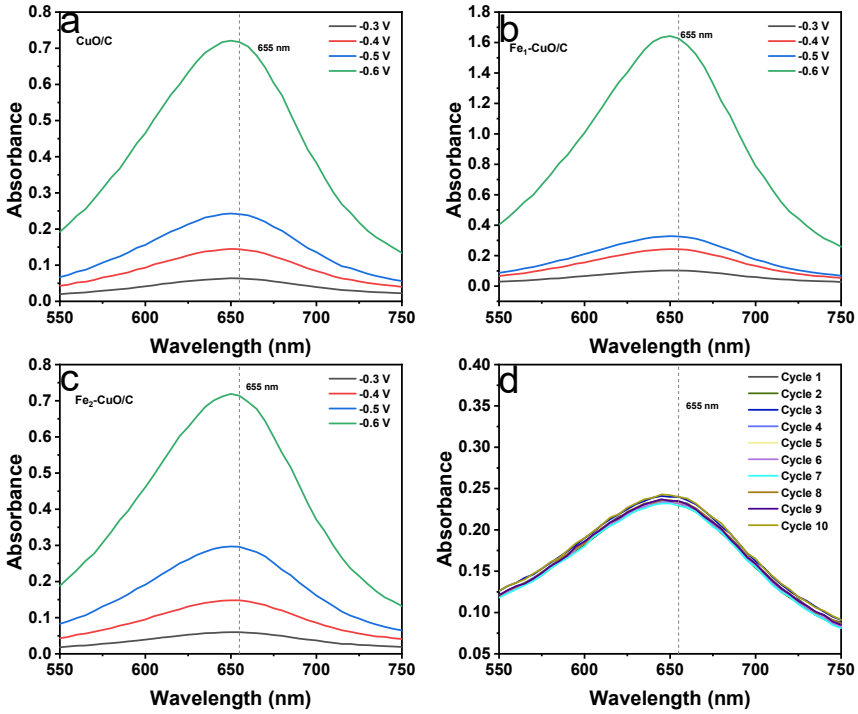

Figure S12. UV-vis absorption spectra of the electrolytes colored with indophenol blue indicator for the quantification of produced NH_4^+.

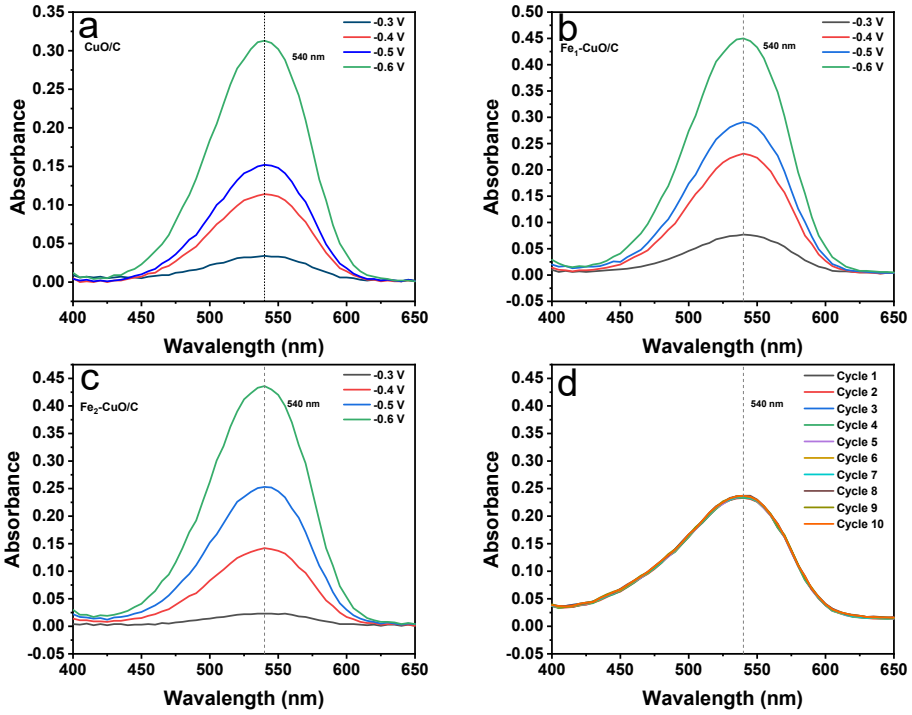

Figure S13. UV-vis absorption spectra of the electrolytes colored with Griess reagent for the quantification of byproduct NO_2^-.

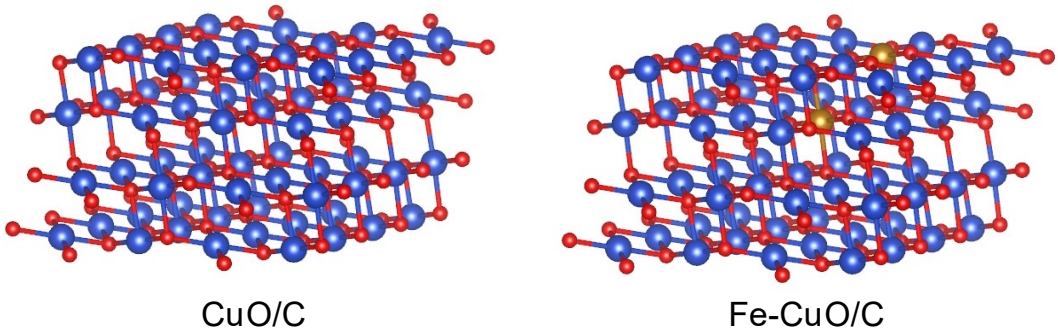

Figure S14. Optimized geometric structures of the CuO/C and Fe-CuO/C catalysts.

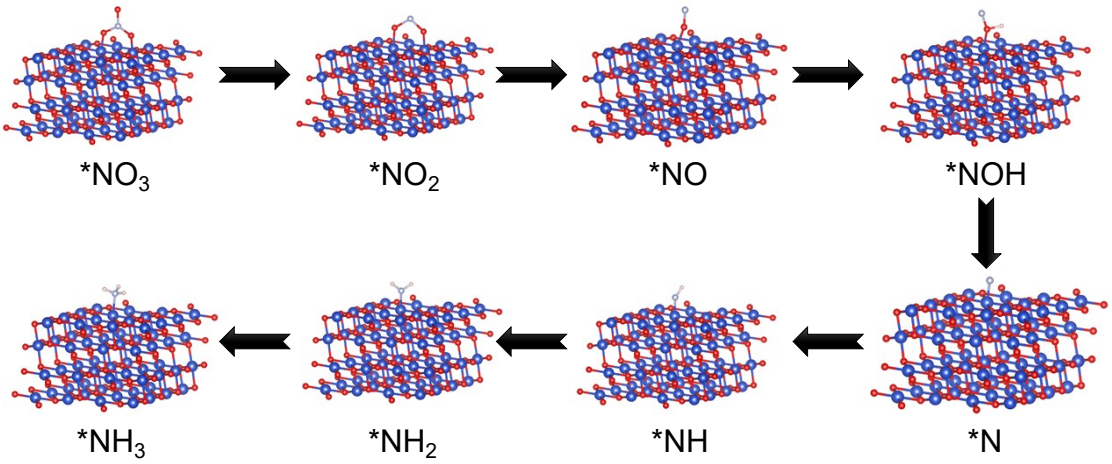

Figure S15. Optimized intermediate structures for the NO_3RR pathway to NH_3 on the CuO/C.

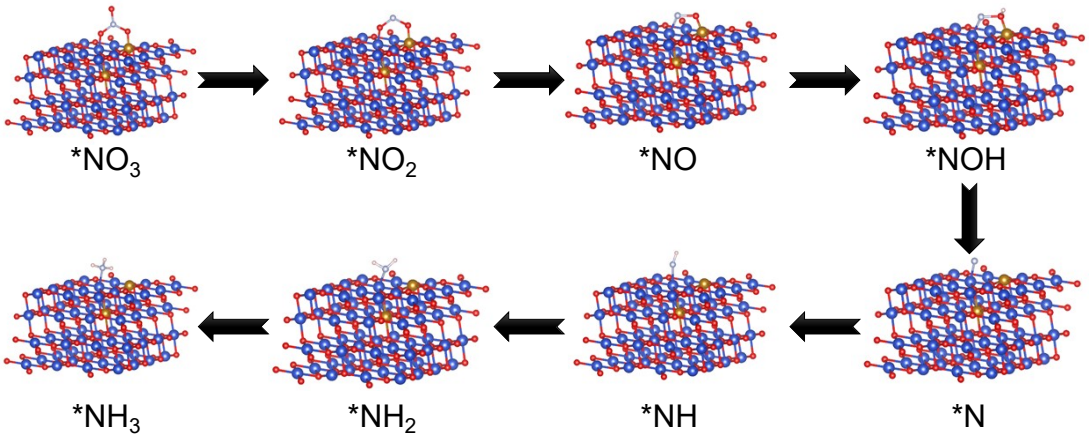

Figure S16. Optimized intermediate structures for the NO_3RR pathway to NH_3 on the Fe-CuO/C .

Table S1 Element contents of obtained electrocatalysts tested by ICP-OES.

Catalysts	Fe/(mg/L)	Cu/(mg/L)	Fe wt.%	Cu wt.%
Fe_1-CuO/C	0.7317	11.470	1.8515%	29.0233%
Fe_2-CuO/C	1.30	11.30	3.28%	28.60%

Measured concentration in the diluted solution.Calculated based on the sample mass of 0.0494 g and the constant volume.

Table S2

Comparison of electrocatalytic nitrate reduction performances (Ammonia formation rate, Current density, FE_{NH3}) of the Fe_1-CuO/C catalyst with recently reported catalysts.

Catalysts	Ammonia formation rate (mg h^{-1} cm^{-2})	$FE_{(NH3+NO2)}$ (%)	Reference
Fe_1-CuO/C	69.19	71.3	This study
$Cu_2O/Cu(OH)_2$	1.63066	76.95	1
MoO_2/C	4.8385	30	2
Mo_2C NSs	25.2	81.4	3
Cu clusters/TiO_2-x	6.11505	81.34	4
CuPc/CeO_2	0.06206	33	5
PdNA on NF	21.28	78	6
PdND@Zr-MOF	4.884	58.1	7
SV-MoS_2	0.11133	78.04	8

References

[1]. J. Geng, S. Ji, *Nano Res.*, 2024, **17**, 4898.

[2]. X. Zhong, X. P. Wu, Y. Liu, S. Q. Yang, H. D. Li, Q. Wang, D. H. Shang, F. Du, A. H. Yuan, F. Yang, *J. Environ. Chem. Eng.*, 2024, **12**, 111871.

[3]. D. Zhu, G. Li, X. Yan, C. Geng, L. Gao, Sci. Total Environ., 2023, 878, 163145.

[4]. X. Zhang, C. Wang, Y. Guo, B. Zhang, Y. Wang, Y. Yu, *J. Mater. Chem. A*, 2022, **10**, 6448.

[5]. X. Li, W. Fan, Y. Bai, Y. Liu, F. Wang, H. Bai, W. Shi, *Chem. Eng. J.*, 2022, **433**, 133225.

[6]. H. Guo, M. Li, Y. Yang, R. Luo, W. Liu, F. Zhang, C. Tang, G. Yang and Y. Zhou, Small, 2023, **19**, 2207743.

[7]. M. Jiang, J. Su, X. Song, P. Zhang, M. Zhu, L. Qin, Z. Tie, J. L. Zuo and Z. Jin, Nano Lett., 2022, **22**, 2529-2537.

[8]. W. Zheng, L. Zhu, Z. Yan, Z. Lin, Z. Lei, Y. Zhang, H. Xu, Z. Dang, C. Wei, C. Feng, *Environ. Sci. Technol.*, 2021, **55**, 13231–13243.